Available online at www.sciencedirect.com
SCIENCE DIRECT®
International Journal of Heat and Mass Transfer 48 (2005) 5323–5337
International Journal of HEAT and MASS TRANSFER
www.elsevier.com/locate/ijhmt

Periodic state of fluid flow and heat transfer in a lid-driven cavity due to an oscillating thin fin

Xundan Shi [1], J.M. Khodadadi *

Mechanical Engineering Department, Auburn University, 201 Ross Hall Auburn, AL 36849-5341, USA

Received 18 January 2005; received in revised form 15 July 2005
Available online 3 October 2005

Abstract

Results of a computational study of periodic laminar flow and heat transfer in a lid-driven square cavity due to an oscillating thin fin are presented. The lid moves from left to right and a thin fin is positioned normal to the right stationary wall. The length of the fin varies sinusoidally with its mean length and amplitude equal to 10% and 5% of the side of the cavity, respectively. Two Reynolds numbers of 100 and 1000 for a $Pr = 1$ fluid were considered. For a given convection time scale (t_{conv}), fin's oscillation periods (τ) were selected in order to cover both slow ($TR = \tau/t_{conv} > 1$) and fast ($\tau/t_{conv} < 1$) oscillation regimes, covering a Strouhal number range of 0.005–0.5. The periodic flow field for the case with $Re = 1000$ and $TR = 10$ is distinguished by the creation, lateral motion and subsequent wall impingement of a CCW rotating vortex within the lower half of the cavity. Periodic flow and thermal fields of the other nine cases studied were not as varied. Phase diagrams of the stream function and temperature vs. fin's length clearly exhibit the synchronous behavior of the system. Amplitude of fluctuations of the kinetic energy and temperature are very intense near the fin. As the fin oscillates slower, a greater portion of the cavity exhibits intense fluctuations. For slow to moderate oscillations, the maximum value of K_{amp} is observed to be greater for $Re = 1000$ in comparison to $Re = 100$. For fast oscillations, this behavior is reversed. The maximum values of the amplitude of fluctuations of temperature increase monotonically as the fin oscillates slower. The maximum values of θ_{amp} are greater for $Re = 1000$ compared to $Re = 100$. The amplitude of fluctuations of the mean Nusselt number on four walls increase as the fin oscillates slower.

1. Introduction

Modification and control of flow and heat transfer in a rectangular cell by introducing vertical or horizontal plate fins is a viable approach in various engineering applications. Laminar natural convection in differentially heated cavities with internal fins (partitions) has been studied extensively, for example [1] among others. High packaging density and increasing heat flux from electronic modules have necessitated the use of forced convection in electronic cooling practices. Presence of chips or boards in a rectangular cell could have significant effect on the resulting flow field and heat transfer. Besides being a simple benchmark geometry for study of complex flow phenomena, a cavity system can simulate a lubricating groove between sliding plates

* Corresponding author. Tel.: +1 334 844 3333; fax: +1 334 844 3307.
E-mail addresses: shixundan@yahoo.com (X. Shi), khodajm@auburn.edu (J.M. Khodadadi).
[1] Graduate Student, Currently a Lead Research Scientist with Chevron Energy Technology Company, San Ramon, CA 94583, USA.

0017-9310/$ - see front matter © 2005 Elsevier Ltd. All rights reserved.
doi:10.1016/j.ijheatmasstransfer.2005.07.026

Nomenclature

l_p	length of the fin, m
L_p	dimensionless length, i.e. l_p/H
$\overline{Nu}$	average or mean Nusselt number, defined by Eq. (10)
T_c	temperature of the left, bottom and right walls, K
T_h	temperature of the moving lid, K
U_{lid}	velocity of the moving lid, m/s

Greek symbols

θ	dimensionless temperature, i.e. $(T - T_c)/(T_h - T_c)$
τ	period of oscillation, s

Subscripts

b, l, r, t	related to the bottom, left, right and top walls

or approximate the separated flow in a surface cavity with an external stream flowing over it. A great number of studies have focused on this problem and an excellent review paper was recently reported by Shankar and Deshpande [2]. The authors [3] have reported results of a parametric study of steady laminar flow and heat transfer within a lid-driven square cavity due to a single thin fin. Fins with lengths of 5%, 10% and 15% of the side, positioned at 15 locations on the stationary walls were examined for $Re = 500$, 1000, 2000 and $Pr = 1$. Placing a fin on the right wall brings about multi-cell recirculating vortices compared to the case without a fin that exhibits a primary vortex and two small corner cells rotating opposite to the primary vortex. A fin positioned near the top right corner of the cavity can reduce heat transfer most effectively. Placing a fin on the right wall-compared to putting a fin on the left and bottom walls-can always enhance heat transfer on the left wall and at the same time, reduce heat transfer on the bottom, right and top walls.

In light of the extensive work on steady-state behavior of stationary thin fins in various geometries and in a square lid-driven cavity [3] in particular, the next challenge is to study the transient evolution and periodic characteristics of a cavity with an *oscillating* thin fin. Because of the limitation on computing capacity, this topic is still untouched by most researchers. The transient behavior of laminar flow and heat transfer within a lid-driven square cavity due to an oscillating thin fin has been reported by the authors [4]. The lid moves from left to right and a thin fin positioned perpendicular to the right stationary wall oscillates in the horizontal direction. The length of the fin varies sinusoidally with its mean length and amplitude equal to 10% and 5% of the side of the cavity, respectively. Two Reynolds numbers of 100 and 1000 with a $Pr = 1$ fluid were considered. For a given convection time scale (t_{conv}), fin's oscillation periods (τ) were selected in order to cover both slow ($\tau/t_{conv} > 1$) and fast ($\tau/t_{conv} < 1$) oscillation regimes. This corresponded to a Strouhal number range of 0.005 to 0.5. The number of the cycles needed to reach the periodic state for the flow and thermal fields increases as τ/t_{conv} decreases for both *Re* numbers with the thermal field attaining the periodic state later than the velocity field. The key feature of the transient evolution of the fluid flow for the case with $Re = 1000$ with slow oscillation is the creation, lateral motion and subsequent wall impingement of a CCW rotating vortex within the lower half of the cavity. This CCW rotating vortex that has a lifetime of about 1.5τ brings about marked changes to the temperature field within a cycle. The dimensionless time for the mean Nusselt numbers to reach their maximum or minimum is independent of the frequency of the fin's oscillation and dependent on the distance between the oscillating fin and the respective wall, and the direction of the primary CW rotating vortex. The phase lag angle between the oscillation of the fin and the mean Nusselt number on the four walls increases as the distance between the fin and the respective wall increases. The periodic state of the flow and thermal fields for the same cavity is discussed here. Some related research relevant to the present study has been reported. Flow and heat transfer in a channel due to the presence of very thin fins swinging back and forth normal to the flow direction was investigated by Fu and Yang [5,6]. The Arbitrary Lagrangian–Eulerian (ALE) method was adopted to handle the moving fins. The boundary layers attaching on the fins were contracted and disturbed. The parameters of the velocities of the fluid and the swinging speed of the fins were employed to investigate the evolving flow and thermal fields. Variations of the average Nusselt number on the fin with time for various cases showed that the swinging of the fin results in a significant heat transfer enhancement.

The objective of this study was to elucidate the periodic state of the flow and thermal fields due to an oscillating thin fin attached to a wall of a square lid-driven cavity. Given the existing thorough knowledge of the steady 2-D laminar flow in lid-driven cavities, it is appropriate that the effect of an oscillating fin on the flow and thermal fields first be elucidated for such a system. In addition to complementing [4], knowledge of the periodic state of the fluid flow, temperature fields, kinetic energy and Nusselt numbers on the four walls are the key elements in design of similar systems.

2. Problem formulation

The physical model for a 2-D lid-driven cavity (height H and length L) is shown in Fig. 1a. For the present study it is assumed that $H = L$ and the top wall is moving at the speed of U_{lid} from left to right, whereas the remaining three walls are stationary. The moving wall is maintained at a temperature (T_h) different from the remaining walls of cavity (T_c), with $T_h > T_c$. Based on the earlier findings of the authors [3], a thin fin is attached to the middle of the right wall. The fin is made of a highly-conductive material, so the Biot number is much smaller than 1. The fin can move back and forth horizontally and its length is

$$l_p = l_m + l_o \sin 2\pi ft, \tag{1}$$

where f is the frequency of the fin's oscillation. Fig. 1b shows the time dependent variation of the length of the fin, with the period of oscillation τ equal to $1/f$. The dimensionless horizontal velocity of the fin is

$$U_p = \frac{u_p}{U_{lid}} = -2\pi \cdot \frac{l_o f}{U_{lid}} \cdot \cos 2\pi ft = -2\pi \cdot St \cdot \cos 2\pi ft, \tag{2}$$

where $St = l_o f / U_{lid}$ is the Strouhal number. The vertical velocity of the fin is zero. The effect of natural convection is neglected, so the ratio Gr/Re^2 is taken to be much smaller than 1.

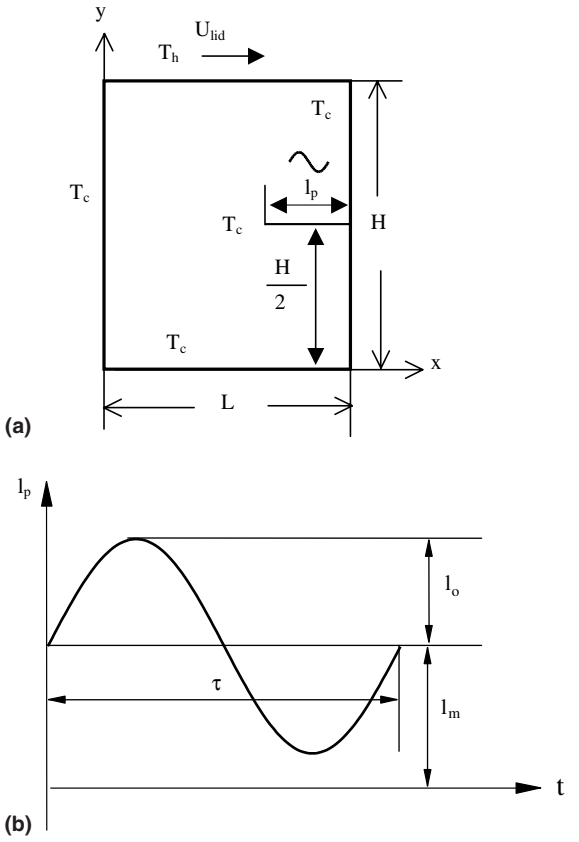

Fig. 1. Model of a square lid-driven cavity: (a) geometry and the coordinate system, and (b) oscillating length of the fin.

2.1. Dimensionless form of the governing equations

The fluid is incompressible with constant properties. Assuming laminar flow, gravity effect and viscous dissipation are neglected. Using the cavity height, lid velocity and the two extreme temperatures as reference scales, the governing equations of continuity, momentum and thermal energy are written in dimensionless form

$$\nabla \cdot \bar{V} = 0, \tag{3}$$

$$\frac{\partial \bar{V}}{\partial t^*} + \bar{V} \cdot \nabla \bar{V} = -\nabla P + \frac{1}{Re} \nabla^2 \bar{V}, \tag{4}$$

$$\frac{\partial \theta}{\partial t^*} + \bar{V} \cdot \nabla \theta = \frac{1}{RePr} \nabla^2 \theta, \tag{5}$$

with Re and Pr equal to $U_{lid} H/\nu$ and ν/α, respectively. For $t^* > 0$, the boundary conditions are

$$\begin{aligned} &\text{At } X = 0, 1 \quad \text{and} \quad Y = 0: \quad U = V = 0,\ \theta = 0, \\ &\text{At } Y = 1: \quad U = 1,\ V = 0,\ \theta = 1, \\ &\text{On the moving fin}: \quad U = -2\pi St \cos(2\pi ft),\ V = 0,\ \theta = 0. \end{aligned} \tag{6}$$

Therefore, Re, Pr and St are the dimensionless groups that govern this problem. The Reynolds numbers of 100 and 1000 were studied and the Prandtl number of the fluid is fixed to 1. Given the results of [3], l_m and l_o were assigned $0.1H$ and $0.05H$, respectively. As for the range of the St studied, one needs to focus on the dominating time scales in this problem and the relationship of the frequency of oscillation in comparison to these time scales. The time scales for convection and diffusion are given as:

Table 1
Number of cycles needed to reach the periodic states for fluid flow (N_f) and temperature fields (N_t)

	N_f, N_t				
	$St = 0.5$ (TR = 0.1)	$St = 0.1$ (TR = 0.5)	$St = 0.05$ (TR = 1)	$St = 0.025$ (TR = 2)	$St = 0.005$ (TR = 10)
$Re = 100$	8, 13	6, 8	4, 5	3, 4	3, 3
$Re = 1000$	64, 95	52, 56	31, 35	20, 28	7, 11

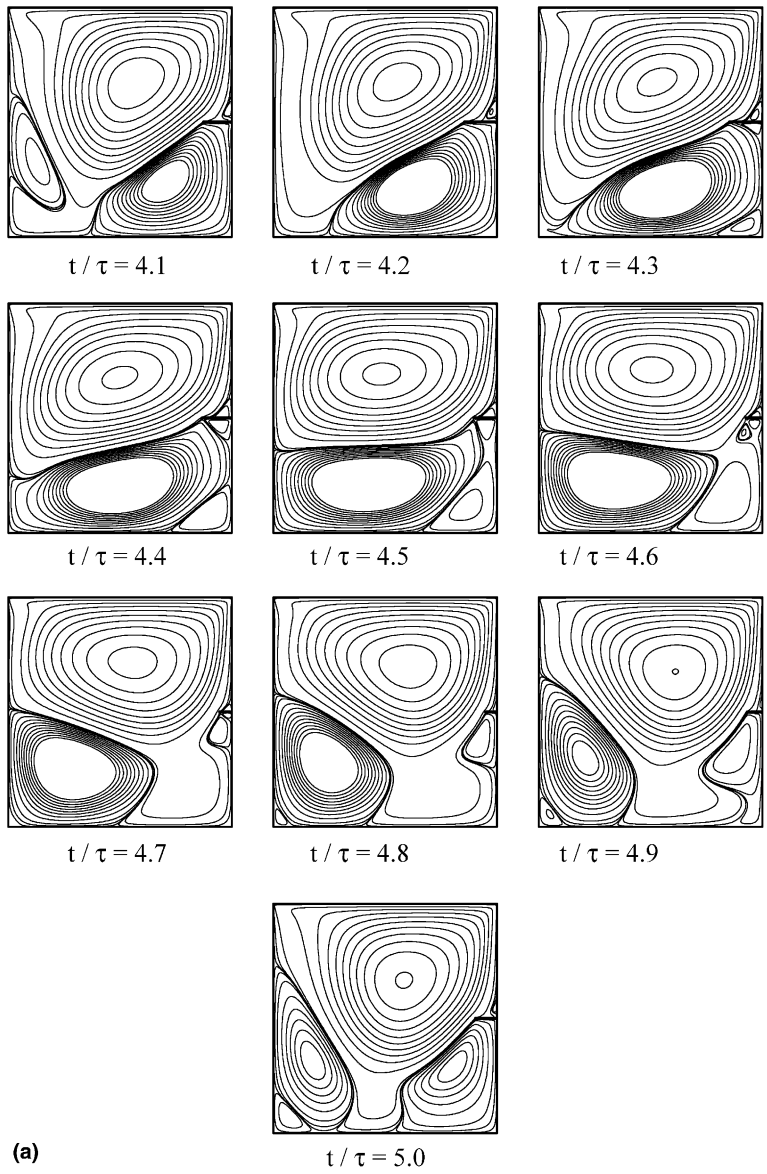

Fig. 2. Periodic flow fields for $Re = 1000$ for (a) TR = 10 and (b) TR = 0.1.

$$t_{\text{conv}} = \frac{H}{U_{\text{lid}}} \quad \text{and} \quad t_{\text{diff}} = \frac{H^2}{\nu}. \tag{7}$$

The ratio of t_{diff} over t_{conv} equals Re. The ratio of the period of the fin's oscillation τ over t_{conv} is defined as TR. TR bigger than 1 corresponds to *slow oscillation*, whereas TR smaller than 1 signifies *fast oscillation*. Note that

$$\text{TR} = \frac{\tau}{t_{\text{conv}}} = \frac{U_{\text{lid}}}{f \cdot H} = \frac{l_{\text{o}}}{H}\frac{1}{St}. \tag{8}$$

With $l_{\text{o}}/H = 0.05$, TR values of 10, 2, 1, 0.5 and 0.1 were investigated that correspond to Strouhal numbers of 0.005, 0.025, 0.05, 0.1 and 0.5, respectively.

2.2. Computational details

The unsteady governing equations were solved by the finite-volume-method using Patankar's [7] SIMPLE algorithm. A 2-D uniformly-spaced staggered grid system was used. Hayase et al.'s [8] QUICK scheme was utilized for the convective terms, whereas the central dif-

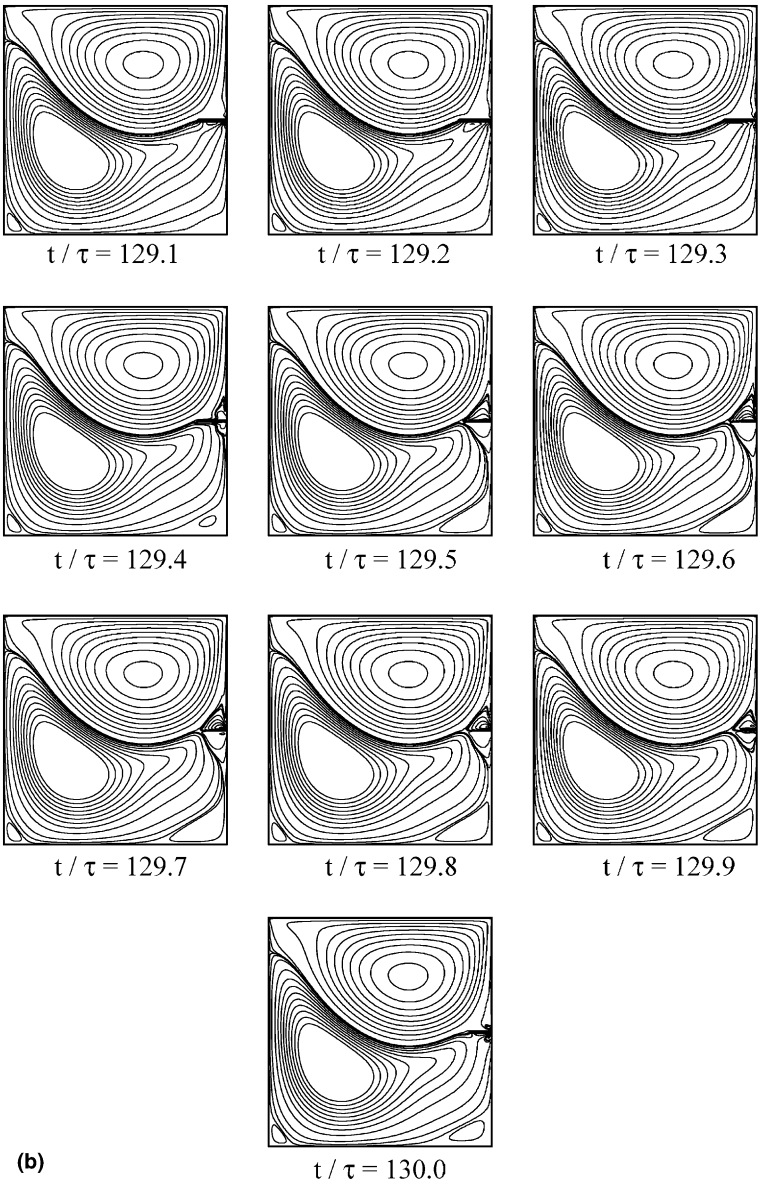

Fig. 2 (*continued*)

ference scheme was used for the diffusive terms. In order to keep consistent accuracy over the entire computational domain, a third-order-accurate boundary condition treatment suggested by Hayase et al. [8] was adopted. The moving fin is within the calculation domain and the FAVOR method (Hirt and Sicilian [9] and Tsukiyama et al. [10]) was used to treat it in this problem. In regard to the computational implementation, the thickness of the fin is zero. Details of a grid independence test using seven different grid densities (40×40, 60×60, 80×80, 100×100, 120×120, 150×150 and 240×240) was given by Shi and Khodadadi [3] for the steady version of this problem. The code was tested and verified extensively via comparing the results with benchmark problems [3,11]. Upon comparing critical quantities and considering both the accuracy and the computational time, the present calculations were all performed with a 150×150 uniformly-spaced grid system. Steady flow and temperature fields of a lid-driven cavity with a fin of length l_m that is attached to the middle of the right wall [3] are treated as the initial fields. For the unsteady computations, tolerance of the normalized residuals upon convergence is set to 10^{-6} for every calculation case. The under-relaxation parameters

for U, V, and θ are all set to 0.6, whereas this parameter for pressure correction is set to 0.3. The three-time-level-method that is a 2nd order implicit scheme is used for approximating the unsteady terms. After conducting a time step independence test [4,11], the time step $\Delta t = \tau/100$ was used.

3. Results and discussions

The mean and oscillating lengths of the fin were $l_m/H = 0.1$ and $l_o/H = 0.05$, respectively. For $t < 0$, the fin's length was equal to l_m/H. For $t \geqslant 0$, the length of the thin fin varies according to Eq. (1). After a certain period of time, the fluid flow and temperature fields will reach their periodic states. The evolution of the fluid flow and temperature fields and the transient response of the average Nusselt numbers on the four walls were discussed in [4]. Adopting a very stringent criteria [11], the number of cycles needed to reach the periodic state (N_f and N_t) are summarized in Table 1. Comparing the $Re = 100$ and 1000 cases, it was observed that it takes fewer cycles to reach the periodic state for the lower Re. For a given Re, it took more cycles to reach the periodic state when TR is smaller (i.e. Strouhal number is greater). For all the cases investigated, it takes fewer

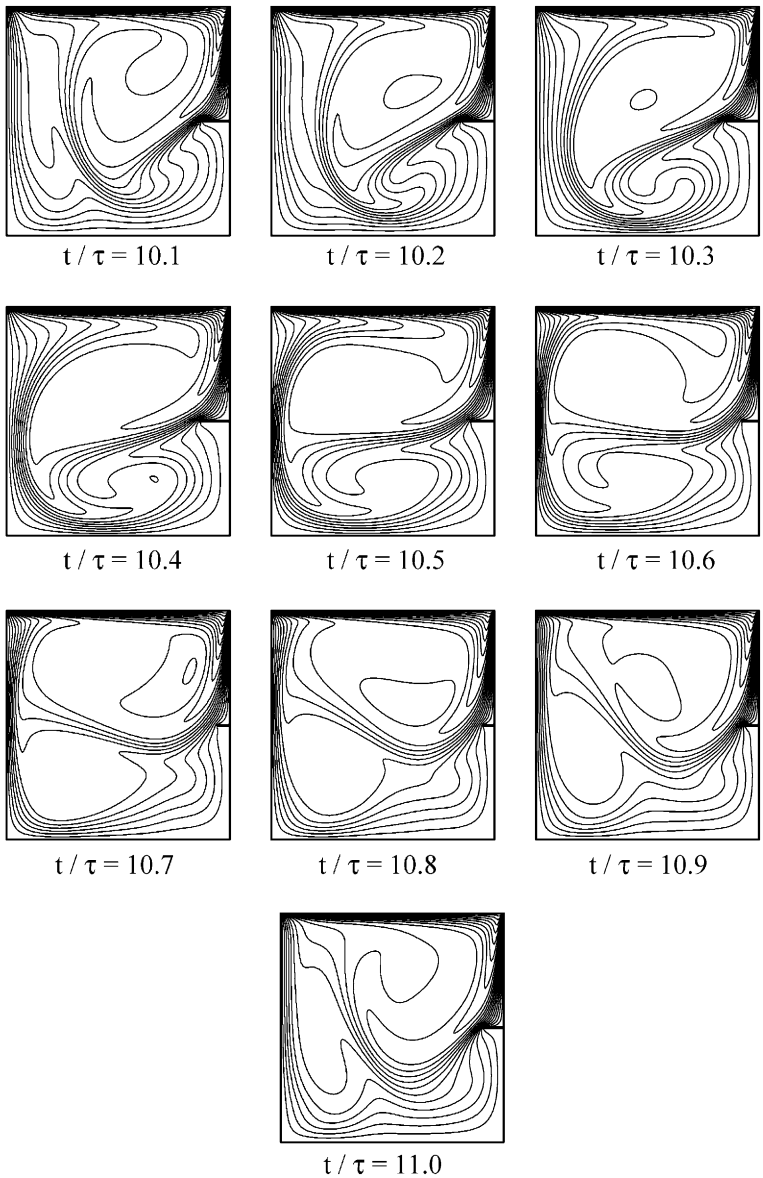

Fig. 3. Periodic temperature fields for $Re = 1000$ and TR = 10 (contour level increment of 0.05).

cycles for the flow field to reach the periodic state in comparison to the temperature field. The difference between N_t and N_f increases as TR decreases. The periodic fields, phase diagrams for ψ and θ, amplitude of fluctuations of spatially averaged kinetic energy density K_{amp}, amplitude of fluctuations of the dimensionless temperature, θ_{amp} and amplitude of fluctuations of the average Nusselt number on the four walls are discussed in this paper.

3.1. Periodic flow and temperature fields

The periodic flow fields for $Re = 1000$ and TR = 10 (slow oscillation) are given in Fig. 2a. Upon attaining the periodic state, the most remarkable feature of this flow field within a cycle is the emergence, lateral motion, wall impingement and disappearance of the CCW rotating vortex within the lower half of the cavity. The lifetime of this CCW rotating vortex is about one and a half period of the fin's oscillation. This implies that the emergence, movement and disappearance of this CCW rotating vortex are closely dependent on the oscillation of the fin. Since the lifetime of the CCW vortex is greater than the period of the motion of the fin, there are generally two CCW vortices within the lower half of the cavity at a given instant. These two CCW vortices can be found at different stages of their lifetime. The cycle-to-cycle changes of the flow field of the other nine cases studied were not as varied as the case detailed above. For example, for the case of $Re = 100$ and TR = 10, a similar CCW rotating vortex was observed in the lower half but its spatial coverage was much smaller and the vortex never impinged on the left wall. The periodic flow fields for fast oscillations (TR < 1) did not exhibit marked changes during the cycle. The periodic flow fields for such a situation are shown in Fig. 2b for $Re = 1000$ and TR = 0.1. It is observed that the oscillating fin only affects the area near the fin. The primary CW vortex in the upper half and the CCW vortex in the lower half exhibit little change during the cycle and appear to be frozen in time. Comparing the flow fields for fast oscillations (TR < 1) to steady flow fields corresponding to the extreme lengths of the fin studied [3], spectacular resemblance is observed for the cases $L_p = l_p/H = 0.1$ and 0.15. Similar trends for the behavior of mean Nusselt numbers for cases of fast oscillations prompted the authors [4] to set forth the notion of an *equivalent* length, defined as the length of a fixed fin for a system under steady-state condition that has the same mean Nusselt number of a system with an oscillating fin when t approaches infinity. Extending such a notion for flow fields, we can conclude that as the fin oscillates faster, its *equivalent* length increases and a pseudo-steady flow field similar to the steady state is established.

The periodic temperature fields for the $Re = 1000$ and TR = 10 case are shown in Fig. 3. The temperature distribution in the lower half of the cavity depends on the cyclic creation and movement of the CCW rotating vortex that is formed near the oscillating fin and the right wall within the third quarter of the cycle. Since both the fin and the right wall are cold, the temperature within the CCW rotating vortex is also low. But during the lateral movement of the vortex, the CCW vortex is in contact with the CW rotating primary vortex above it and absorbs heat from it. As a result, the temperature in the CCW rotating vortex increases while moving from the right wall to the left wall. When it impinges on the left wall, the local temperature gradient is steepened markedly.

3.2. Phase diagrams for stream function and dimensionless temperature

Phase diagrams are widely used to exhibit the periodicity of a system. In order to study the periodicity of the flow and temperature fields, four points are selected as representative monitored points. The locations of these four points are shown in Fig. 4. Points A (0.6, 0.3) and D (0.1, 0.3) are in the lower half of the cavity on the path of the evolving CCW vortex. Points B (0.9, 0.52) and C (0.9, 0.48) are very close to the fin and thus are heavily affected by its oscillation. The variation of the stream function (ψ) with fin's dimensionless length $L_p = l_p/H$ for $Re = 1000$ at points A and C are shown in Figs. 5 and 6, respectively. A solid circle denotes the value of the stream function at the beginning of the cycle. This point also coincides with the end of the cycle. An arrow is drawn that points to the evolving values of the stream function as time progresses. Notice that the

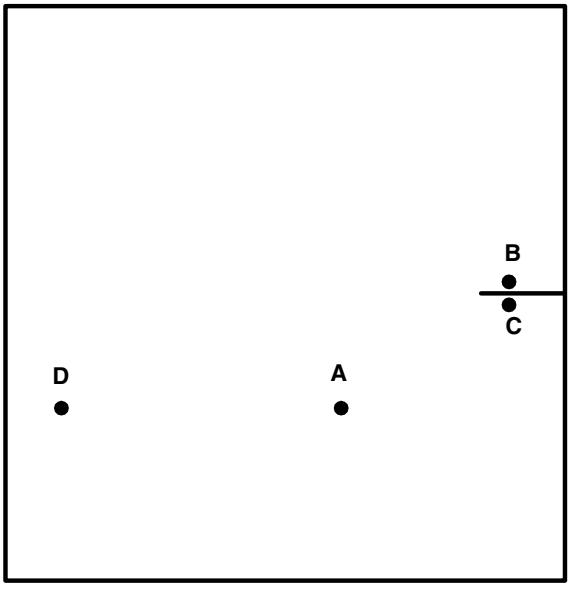

Fig. 4. Locations of the four monitored points A, B, C and D.

phase diagrams are closed loops which may fold a number of times. Recalling the cyclic motion of the CCW rotating vortex within the lower half of the cavity from Fig. 2a for the TR = 10 case, the stream function value changes sign suggesting that point A resides within both CW and CCW rotating vortices. From Fig. 5, one can

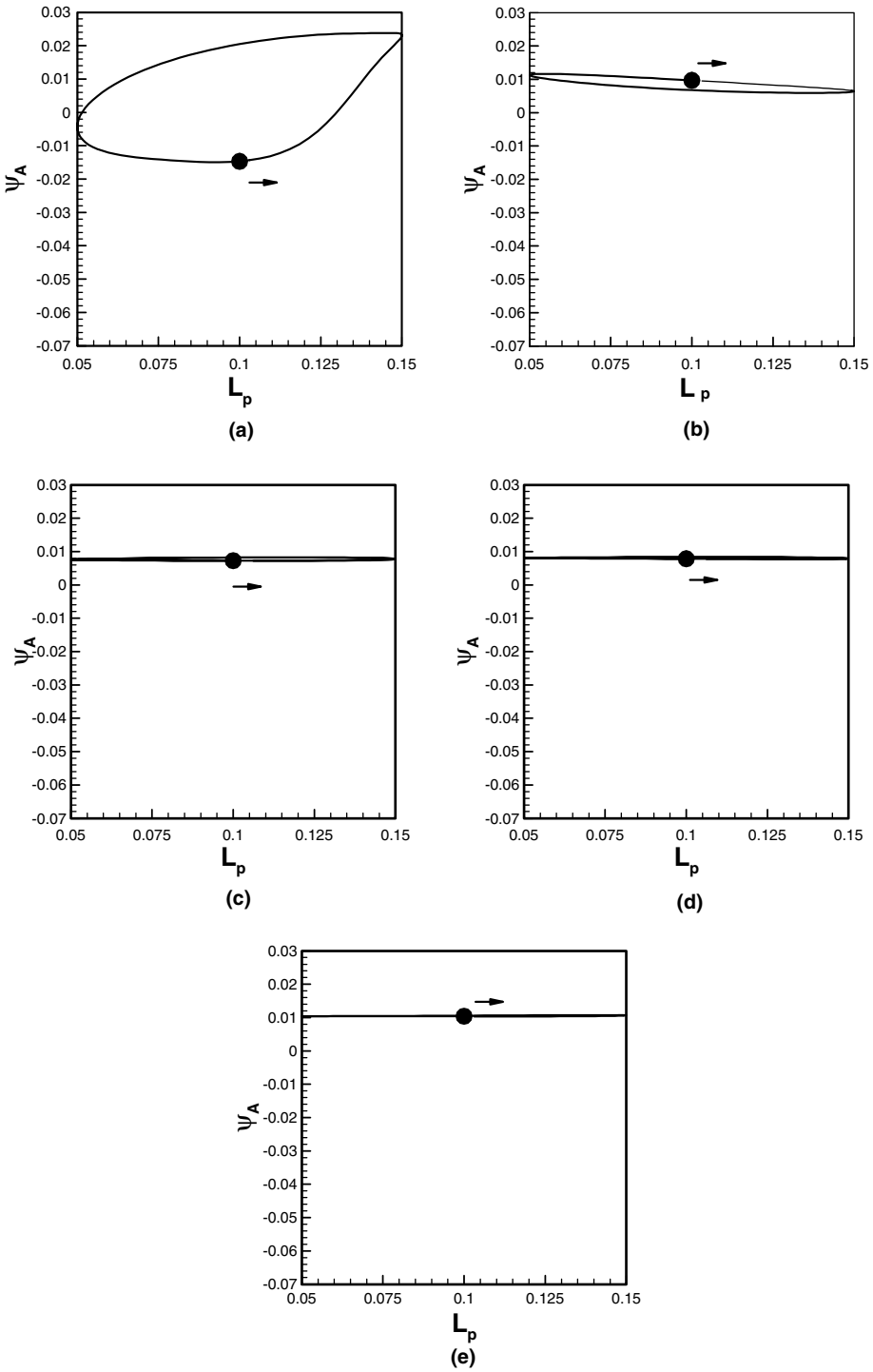

Fig. 5. Stream function vs. L_p phase diagram for point A for $Re = 1000$. (a) TR = 10; (b) TR = 2; (c) TR = 1; (d) TR = 0.5; (e) TR = 0.1.

note that the amplitude of the fluctuation of the stream function at point A decreases drastically as the fin oscillates faster. For all the cases with $Re = 1000$ and TR less than 10, ψ_A values are always greater than zero, implying that point A is always found inside the CCW rotating primary vortex during one period.

As for the stream function phase diagram of point C under the fin that is shown in Fig. 6 for $Re = 1000$, it is

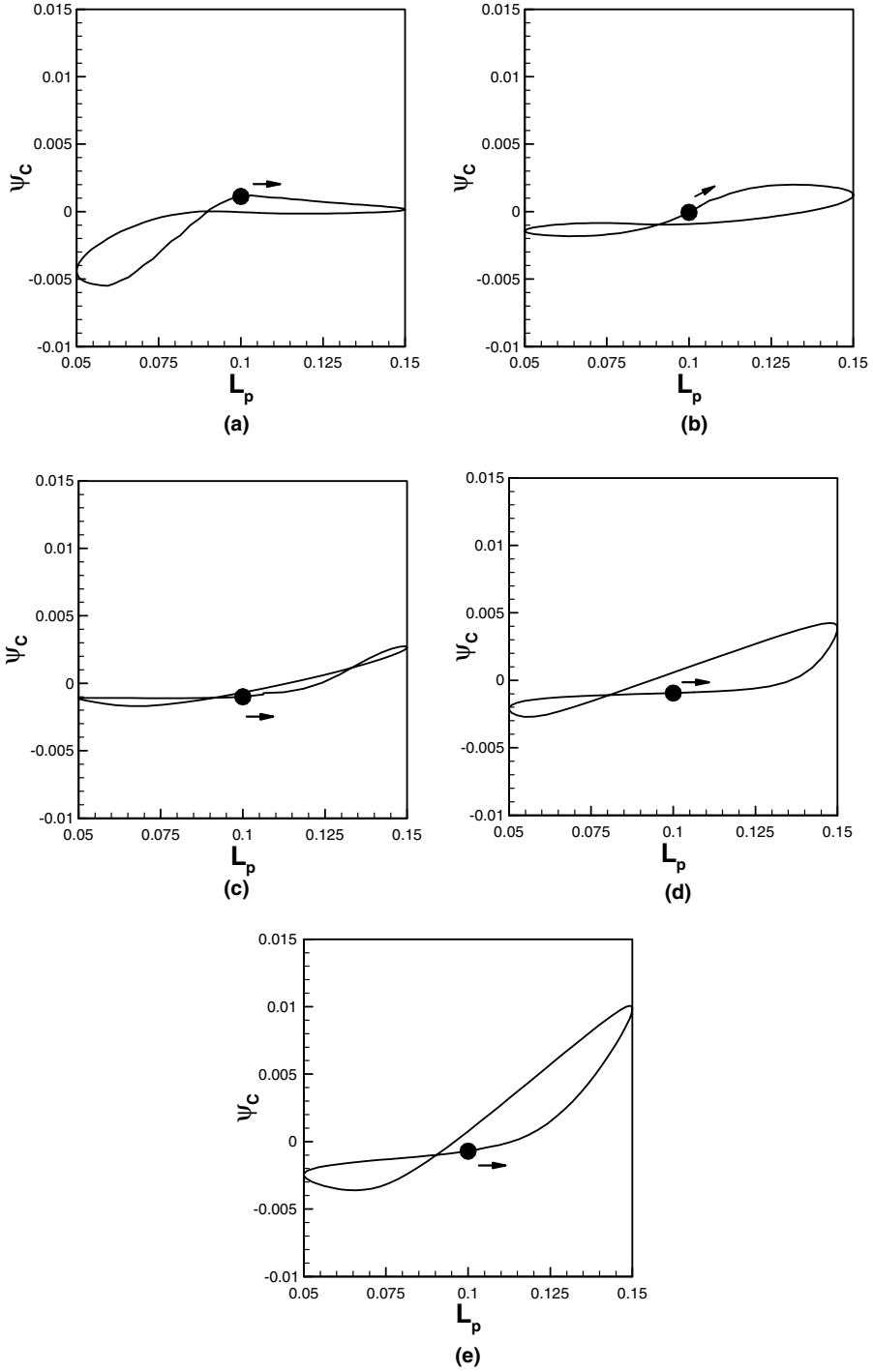

Fig. 6. Stream function vs. L_p phase diagram for point C for $Re = 1000$. (a) TR = 10; (b) TR = 2; (c) TR = 1; (d) TR = 0.5; (e) TR = 0.1.

observed that the fluctuations are enhanced as the fin oscillates faster. It is noticed that ψ_C alternates between positive and negative values. This is because vortices with two different rotating directions are created as the fin elongates and shortens. Similar but less marked trends were observed for point B above the fin [11] for

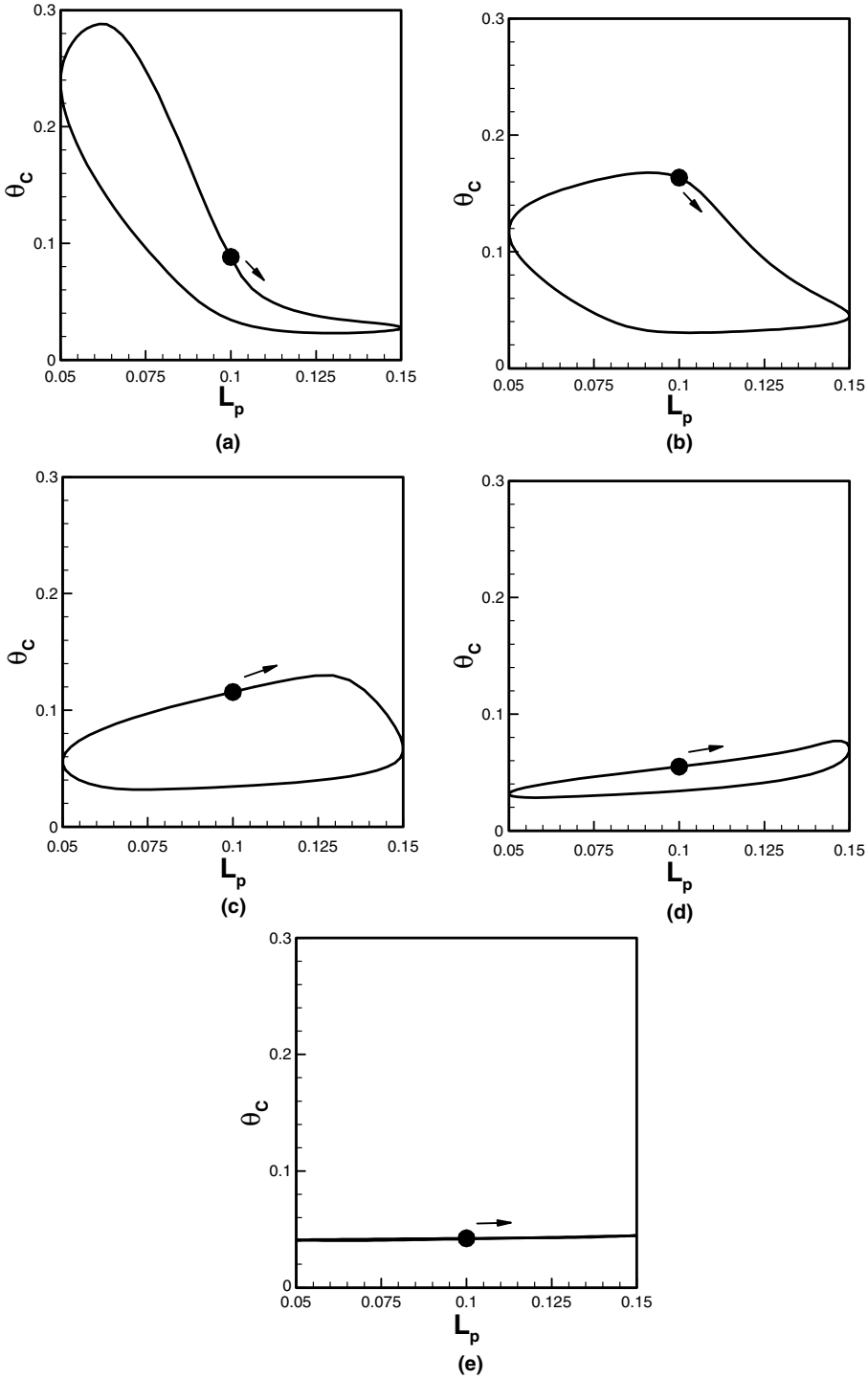

Fig. 7. Dimensionless temperature vs. L_p phase diagram for point C for $Re = 1000$. (a) TR = 10; (b) TR = 2; (c) TR = 1; (d) TR = 0.5; (e) TR = 0.1.

both *Re* numbers. The amplitude of fluctuations at point D that is located near the left wall reduces as TR decreases.

The phase diagrams of dimensionless temperature (θ) vs. fin's dimensionless length (L_p) for $Re = 1000$ at point C are shown in Fig. 7. This case is indicative of all the

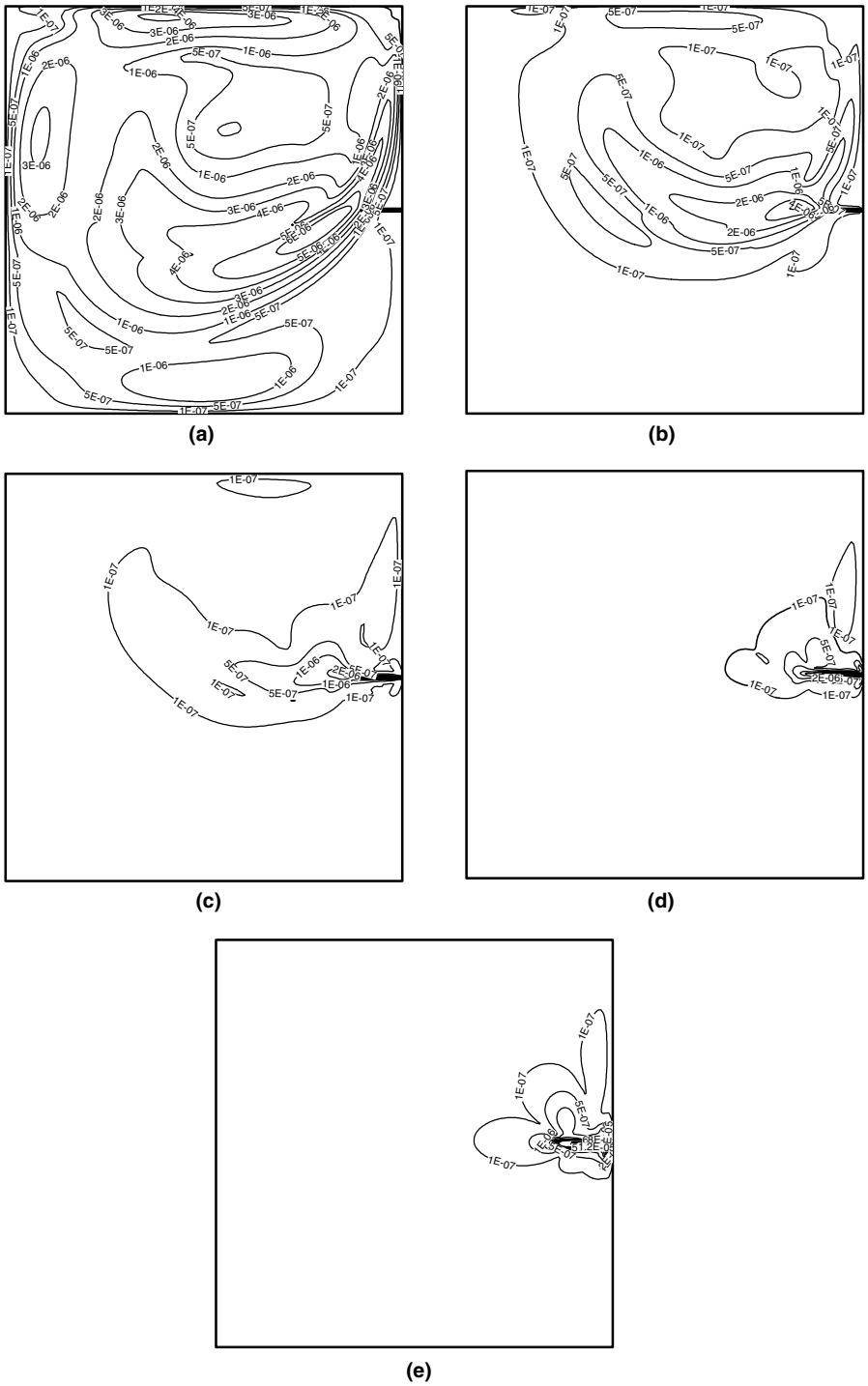

Fig. 8. Contours of the amplitude of fluctuations of kinetic energy for $Re = 1000$. (a) TR = 10; (b) TR = 2; (c) TR = 1; (d) TR = 0.5; (e) TR = 0.1.

cases studied representing most marked variations for the range of TR values studied. Both points B and C experience marked variations of temperature within each cycle in comparison to points A and D. As a matter of fact, the amplitude of fluctuations of θ for TR < 10 at points A and D was negligible [11].

3.3. Amplitude of fluctuations of kinetic energy

In order to investigate how fluid flow in different zones of the cavity is affected by the oscillation of the fin, the dimensionless kinetic energy of every grid cell for every time step is evaluated as follows:

$$K = \iint_{CV} \frac{U^2 + V^2}{2} \mathrm{d}X\,\mathrm{d}Y, \tag{9}$$

where U and V are the dimensionless velocity components in the X and Y directions, respectively. For every grid cell (control volume), K_{amp} is defined as the difference between the maximum and minimum values of K during a period. Fig. 8 shows the contours of K_{amp} for $Re = 1000$. In order to maintain the clarity of the contour fields, contour levels equal to or greater than 10^{-7} are only shown. The areas with greater K_{amp} value are generally concentrated near the fin. The areas near the left and bottom walls are far from the fin and K_{amp} in these areas is very small. For the area near the fin, K_{amp} is greater above the fin than under the fin. This is because the energetic primary vortex that is rotating CW is generally observed within the upper half of the cavity. It was observed that the high-value K_{amp} area for $Re = 100$ expands away from the fin with a slow oscillating fin when TR $\geqslant 1$ and with a fast oscillating fin when TR $\leqslant 1$. For all the cases when $Re = 1000$ (Fig. 8), the high-value K_{amp} area expands monotonically as TR increases. Comparing the results for $Re = 100$ and 1000, one can see that the high-value K_{amp} area is bigger when $Re = 1000$ than $Re = 100$ for TR $\geqslant 1$. But for TR $\leqslant 1$, a reverse trend was observed. Thus, the distribution of K_{amp} not only depends on the period of the fin's oscillation, but also depends on the Reynolds number. Since the maximum K_{amp} is located in the area very close to the fin, it is very hard to distinguish these values in Fig. 8. Fig. 9 shows the variation of maximum values of K_{amp} with TR. The maximum value of K_{amp} is observed to be greater for $Re = 1000$ in comparison to $Re = 100$ for TR $\geqslant 1$. But if TR < 1, the maximum value of K_{amp} is greater when $Re = 100$.

3.4. Amplitude of fluctuations of dimensionless temperature

For every grid point, the amplitude θ_{amp} is defined as the difference between the maximum and minimum values of θ during a period. Fig. 10 shows the contours of the amplitude of fluctuation of dimensionless temperature θ for $Re = 1000$. The zone of high-value θ_{amp} shrinks to a very small area as the fin oscillates faster for both $Re = 100$ and 1000. Higher Reynolds number can help the effects of oscillation of the fin to be transmitted to a wider area. Comparing the shape of the contours in Fig. 10(b) and (c) with the primary CW vortex in Fig. 2a, one can see that the primary vortex plays a very important role on the effects of the oscillation of the fin on the thermal fields. When TR $= 0.1$, the zone of high-value θ_{amp} is very small. This is because the equivalent length of the fin is longer (closer to 0.15) when TR is smaller as we discussed in previous sections. So, the temperature field is not affected appreciably from the oscillation of the fin. Fig. 11 shows the dependence of the maximum values of θ_{amp} on TR. The maximum values of θ_{amp} increase monotonically as TR increases. The maximum values of θ_{amp} are greater for $Re = 1000$ compared to $Re = 100$, except for TR $= 0.1$.

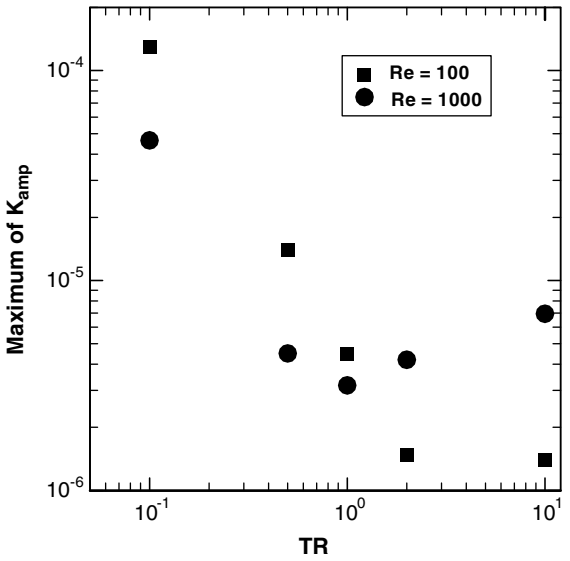

Fig. 9. Maximum value of the amplitude of fluctuations of kinetic energy as a function TR $= \tau/t_{conv}$.

3.5. Amplitude of fluctuations of the mean Nusselt number on four walls

The transient behavior of the mean Nusselt number was discussed by the authors [4] with its definition given as the surface integrals of the instantaneous local Nusselt numbers, i.e.

$$\overline{Nu_i}(t^*) = \int_0^1 Nu_i(s, t^*)\,\mathrm{d}s, \tag{10}$$

with the subscript i denoting b, l, r or t and variable s being X or Y. The amplitude of the oscillations of the mean Nusselt number on the ith wall is defined as:

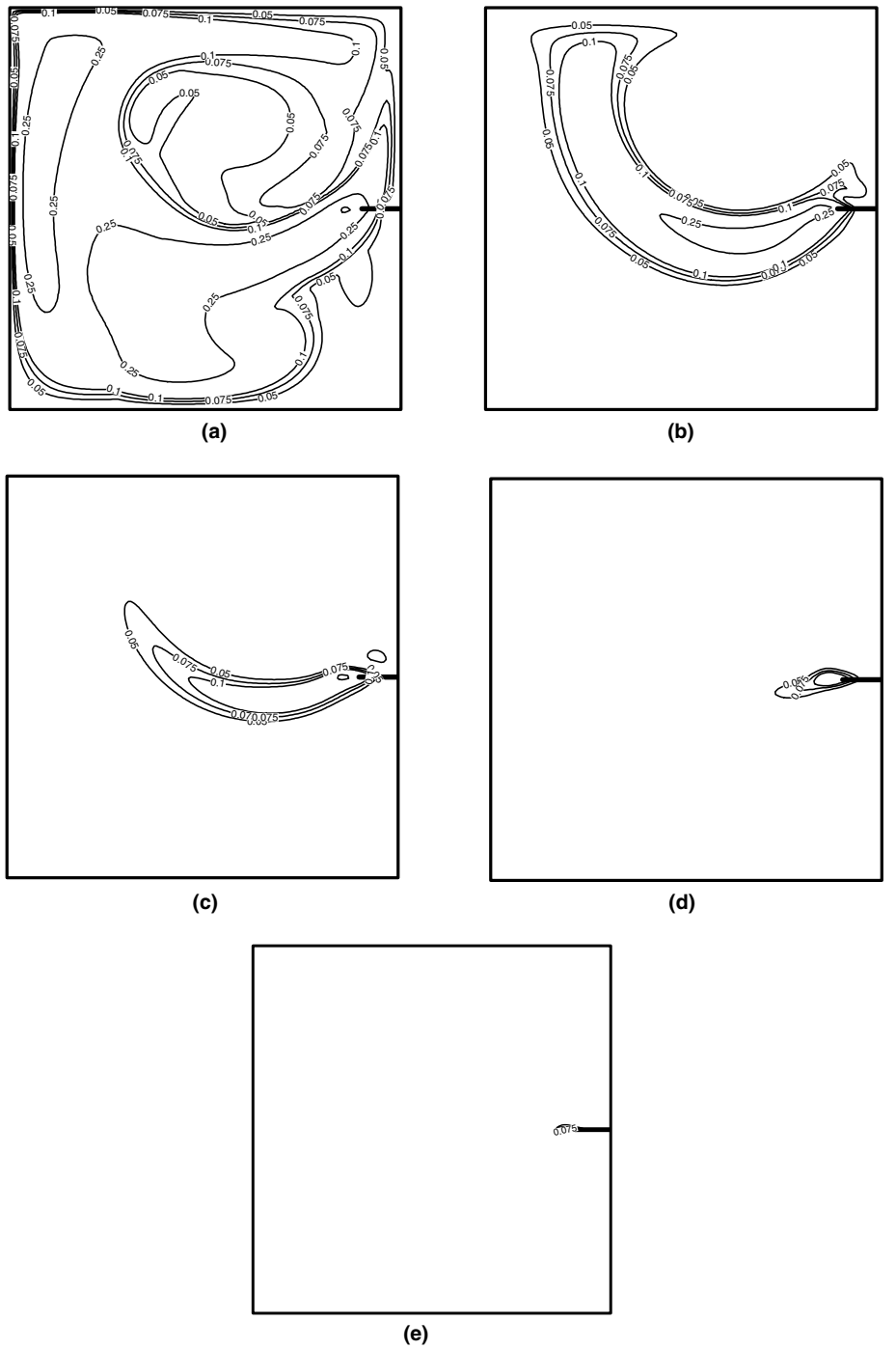

Fig. 10. Contours of the amplitude of fluctuations of dimensionless temperature for $Re = 1000$. (a) TR = 10; (b) TR = 2; (c) TR = 1; (d) TR = 0.5; (e) TR = 0.1.

$$\overline{Nu}_{i\,\mathrm{amp}} = \frac{\overline{Nu}_{i\,\max} - \overline{Nu}_{i\,\min}}{2}, \tag{11}$$

where $\overline{Nu}_{i\,\max}$ and $\overline{Nu}_{i\,\min}$ are the maximum and minimum values of the mean Nusselt number within a period, respectively. Fig. 12 shows the amplitude of fluctuations of the mean Nusselt number on the four walls. In general, the amplitude of fluctuations of the mean Nusselt numbers on all of the four walls exhibit an increasing

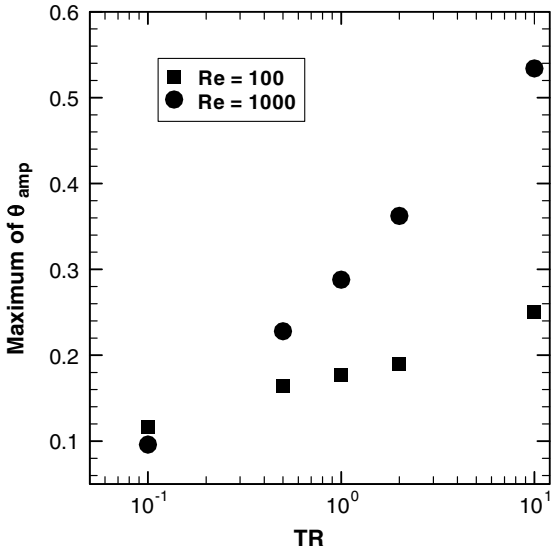

Fig. 11. Maximum value of the amplitude of fluctuations of dimensionless temperature as a function $\mathrm{TR} = \tau/t_{\mathrm{conv}}$.

trend as the fin oscillates slower. Values of $\overline{Nu}_{\mathrm{tamp}}$ and $\overline{Nu}_{\mathrm{lamp}}$ are generally greater when $Re = 1000$ in comparison to the $Re = 100$ case. On the right and bottom walls, the amplitude of fluctuations are much closer to each other.

4. Conclusions

1. The number of the cycles needed to reach the periodic state for the flow (N_{f}) and thermal (N_{t}) fields increases as the fin oscillates faster with $N_{\mathrm{f}} < N_{\mathrm{t}}$.
2. The periodic flow field for the case with $Re = 1000$ and $\mathrm{TR} = 10$ is distinguished by the creation, lateral motion and subsequent wall impingement of a CCW rotating vortex within the lower half of the cavity. This cyclic motion of this vortex brings about marked changes to the temperature field within a period. Periodic flow and thermal fields of the other nine cases studied were not as varied.

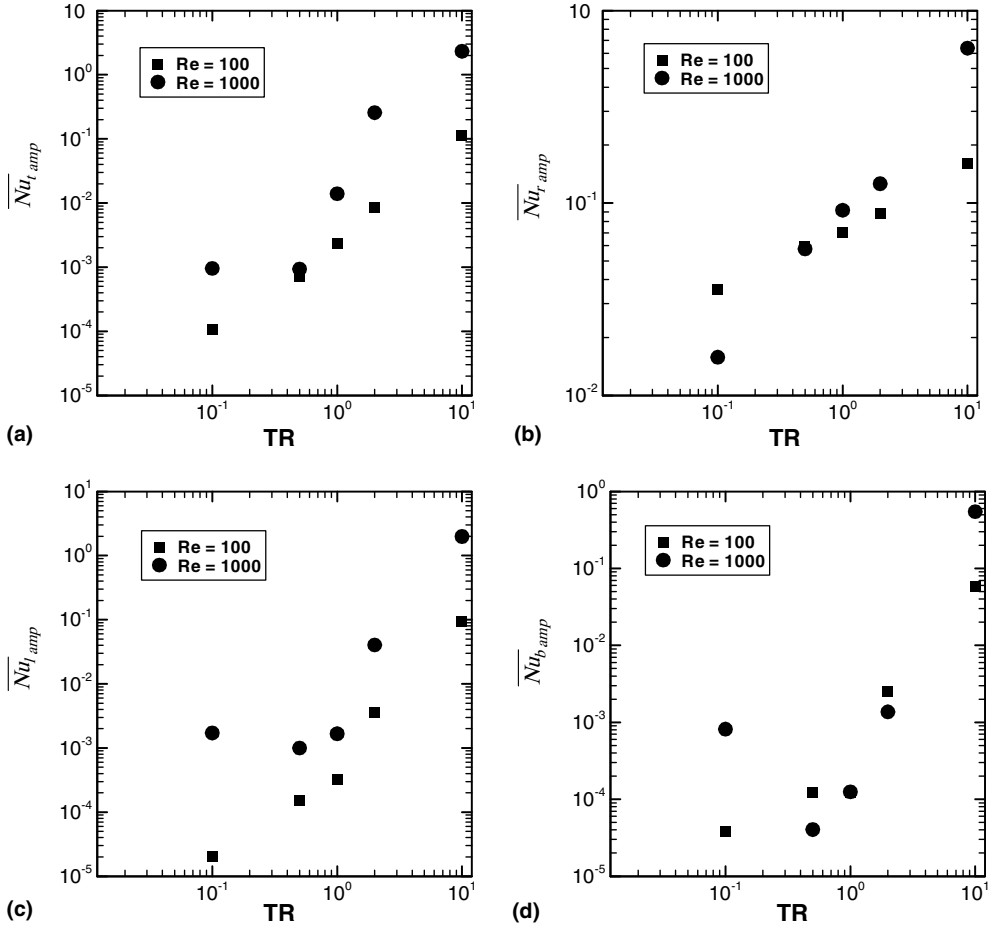

Fig. 12. Amplitude of fluctuations of the mean Nusselt number on four walls: (a) Top wall; (b) right wall; (c) left wall; (d) bottom wall.

3. Phase diagrams of the stream function and dimensionless temperature vs. fin's dimensionless length clearly exhibit the synchronous behavior of the system.
4. Amplitude of fluctuations of the kinetic energy and temperature are very intense near the fin. As the fin oscillates slower, a greater portion of the cavity exhibits intense fluctuations. For slow to moderate oscillations, the maximum value of K_{amp} is observed to be greater for $Re = 1000$ in comparison to $Re = 100$. For fast oscillations, this behavior is reversed. The maximum values of the amplitude of fluctuations of temperature increase monotonically as the fin oscillates slower. The maximum values of θ_{amp} are greater for $Re = 1000$ compared to $Re = 100$.
5. The amplitude of fluctuations of the mean Nusselt number on four walls increase as the fin oscillates slower.

References

[1] Y. Yamaguchi, Y. Asako, Effect of partition wall on natural convection heat transfer in a vertical air layer, J. Heat Transfer 123 (2001) 441–449.
[2] P.N. Shankar, M.D. Deshpande, Fluid mechanics in the driven cavity, Annu. Rev. Fluid Mech. 32 (2000) 93–136.
[3] X. Shi, J.M. Khodadadi, Laminar fluid flow and heat transfer in a lid-driven cavity due to a thin fin, J. Heat Transfer 124 (2002) 1056–1063.
[4] X. Shi, J.M. Khodadadi, Fluid flow and heat transfer in a lid-driven cavity due to an oscillating thin fin: transient behavior, J. Heat Transfer 126 (2004) 924–930.
[5] W.-S. Fu, S.-J. Yang, A new model of heat transfer of fins swinging back and forth in a flow, Int. J. Heat Mass Transfer 44 (2001) 1687–1697.
[6] W.-S. Fu, S.-J. Yang, A numerical study of effects of the swinging amplitude of fins on heat transfer characteristics in a flow, Heat Mass Transfer 38 (2001) 55–63.
[7] S.V. Patankar, Numerical Heat Transfer and Fluid Flow, Hemisphere Pub. Co., Washington, DC, 1980.
[8] T. Hayase, J.A.C. Humphrey, R. Grief, A consistently formulated quick scheme for fast and stable convergence using finite-volume iterative calculation procedures, J. Comput. Phys. 98 (1992) 108–118.
[9] C.W. Hirt, J.M. Sicilian, A porosity technique for the definition of obstacles in rectangular cell meshes, in: Proceedings of the Fourth Int. Conf. Ship Hydrodynamics, Washington, DC, 1985.
[10] H. Tsukiyama, Y. Tajima, M. Yao, H. Arai, Solution method of the time transient moving boundary problems using generalized porous media technique—FAVORITE (FAVOR ImitaTE) program, J. Wind Eng. Industr. Aerodyn. 46–47 (1993) 381–391.
[11] X. Shi, Forced and natural convection heat transfer within enclosures with fixed and moving fins and partitions. Ph.D. Thesis, Department of Mechanical Engineering, Auburn University, 2003.